DOI:
10.1007/978-3-030-00931-1_44

Document Version
Peer reviewed version

Thalamic nuclei segmentation using tractography, population-specific priors and local fibre orientation

Carla Semedo[1], M. Jorge Cardoso[2,1], Sjoerd B. Vos[1,3,4], Carole H. Sudre[2,1,5], Martina Bocchetta[5], Annemie Ribbens[6], Dirk Smeets[6], Jonathan D. Rohrer[5], and Sebastien Ourselin[2]

[1] Centre for Medical Image Computing (CMIC), University College London
[2] School of Biomedical Engineering and Imaging Sciences, King's College London
[3] MRI Unit, Epilepsy Society, Chalfont St Peter
[4] Wellcome EPSRC Centre for Interventional and Surgical Sciences (WEISS), University College London
[5] Dementia Research Centre, Department of Neurodegenerative Disease, Institute of Neurology, University College London
[6] icometrix, Leuven, Belgium

Abstract. The thalamus is a deep grey matter structure that plays an important role in propagating nerve impulses between subcortical regions and the cerebral cortex. It is composed of distinct nuclei that have unique long-range connectivity. Accurate thalamic nuclei segmentation provides insights about structural connectivity and the neurodegeneration mechanisms occurring in distinct brain disorders, for instance Alzheimer's disease and Frontotemporal dementia (FTD). In this work, we propose a novel thalamic nuclei segmentation approach that relies on tractography, thalamic nuclei priors and local fibre orientation. Validation was performed in a cohort of healthy controls and FTD patients against other thalamus connectivity-based parcellation methods. Results showed that the proposed strategy led to anatomical plausible thalamic nuclei segmentations and was able to detect connectivity differences between controls and FTD patients.

1 Introduction

The thalamus is the main gateway of information to the cerebral cortex for: (i) all sensory information, with exception of the olfactory system; (ii) anatomical loops of motor systems, between the cerebellum or basal ganglia and cerebral cortex and (iii) projections from limbic structures to the brain cortex. Additionally, the human thalamus has distinct nuclei that differ in terms of subcortical and cortical neural pathways. These two aspects have led to the development of segmentation techniques to parcellate the thalamus into different nuclei.

Current imaging modalities such as Computed Tomography (CT) and Magnetic Resonance (MR) enable us to identify the thalamus, but they do not provide enough contrast to differentiate between thalamic subnuclei. Conversely,

diffusion MRI, a technique which assesses water diffusion within biological tissues, has emerged as a way of exploring the unique white matter (WM) pathways within each thalamic nuclei and their connections with cortical regions. The majority of thalamus parcellation techniques reported to date rely on diffusion MR data to divide the thalamus into its distinct nuclei, by considering either the local diffusion patterns and/or structural connectivity.

A commonly used thalamus tractography-based procedure was developed by Behrens et al. [1], available as part of FSL[7]. Diffusion data analysis and tractography are done in a combination of standard and native spaces through single atlas propagation, which can affect the biological plausibility of connectivity findings. Furthemore, validation was done in a small cohort of normal controls, but its performance has not been tested when dealing with highly pathological data.

A recent strategy [2] addressed these aspects by performing Diffusion Weighted (DW) data processing and probabilistic tractography in the subject's native space, as well as by integrating population-specific thalamic nuclei priors. This method was able to detect connectivity differences between the thalamus and both the frontal and temporal lobes, which is consistent with previous FTD studies. These results could not be replicated with the FSL pipeline [3].

In this work, we propose to improve on the above mentioned native space based strategy by integrating local fibre orientation information to enhance thalamus parcellations.

All the previously mentioned procedures were evaluated on a population of healthy controls and FTD patients. Results showed that the proposed strategy led to robust thalamic nuclei segmentations and was also sensitive to connectivity changes between controls and FTD patients.

2 Methods

2.1 Data

A group of 55 individuals – participants of a multicentre study – 23 healthy controls (mean age 43.0 years, age range [26.5, 70.6], 16 female) and 32 FTD patients (mean age 50.9 years, age range [20.5, 77.0], 19 female) were considered in this work. Diffusion data consisted of two repeated scans, acquired along 64 non-collinear isotropically distributed directions (b-value of 1000 s/mm^2) and four additional b-0 volumes on 1.5T and 3T Philips, Siemens and GE scanners, with 2.5 mm^3 isotropic voxel size. Volumetric T1-weighted MPRAGE images were also obtained with an isotropic voxel size of 1.1 mm^3.

2.2 Pre-processing

T1 images were corrected for bias field using N4 algorithm [4]. DW images were also corrected for artifacts. First, the DW data was motion- and eddy-current

[7] http://fsl.fmrib.ox.ac.uk/

corrected by affinely registering them to an average b-0 image, generated through a groupwise registration of the b-0 volumes in each subjects data [5]. Secondly, susceptibility artefacts were addressed through phase unwrapping followed by non-linear registration along the phase encoding direction of the distorted DW images to the T1-weighted image [6].

2.3 FSL pipeline

In brief, Behrens et al. work [1] comprised five main steps. First, the thalamus and six cortical regions of interest (ROIs) – prefrontal, motor, sensory, parietal, occipital and temporal cortices – per hemisphere were extracted from an atlas in MNI152 space, available as part of SPM12, which follows the Neuromorphometrics Inc. protocol and includes 135 neuroanatomical labels. Then, all these ROIs were registered from MNI space to each subject's diffusion space by composing the intra-subject affine registration between the mean b=0 volume and T1-weighted data (using the FLIRT algorithm [7]) with a non-linear registration from the T1-weighted image into the atlas in MNI152 space (using the FNIRT algorithm [8]). Third, fibre orientations within the dMRI data were inferred using the Ball-and-Stick model. Fibre architecture between the thalamus and the six cortical ROIs was reconstructed through probabilistic tractography and for each hemisphere separately, using the thalamus as seed region and any of the six cortical ROIs as target region. Here, the connectivity between any two points of interest was defined as the proportion of samples that pass between them. Finally, each thalamic voxel was labelled as the cortical region with the highest connection probability.

2.4 Thalamus parcellation using tractography, population-specific priors and local fibre orientation

2.4.1 Previous work (PW): The basis of the strategy proposed in this study was an existing thalamic nuclei segmentation procedure [2], that succinctly consists in:

1. *Data analysis in subject's space*: Each subject T1-weighted image was parcellated into 143 regions [9]. Thalamus and six cortical regions (prefrontal, motor, sensory, parietal, occipital and temporal cortices) were selected per hemisphere. During DW artefacts correction, the average b-0 volume was registered into the T1-weighted image as one of the steps to correct for susceptibility distortions. The inverse of this transformation was computed and used to map the thalamic and cortical masks from T1 to DW space. Fibre orientations distribution (FOD) were inferred directly from the measured DW signal by using a multi-fibre algorithm constrained spherical deconvolution method [10]. Probabilistic streamline tracking was then performed using the iFOD2 algorithm [11] and repeated for every seed point (thalamus) and target region (any of the six cortical regions), enabling the estimation of the number of streamlines that may exist between them. Finally, a segmentation

of the thalamic nuclei was obtained by estimating the probability that each thalamic voxel was connected to a target cortical ROI.

2. *Population-specific thalamic nuclei priors*: Thalamic nuclei priors were derived through an iterative strategy. First, a population-specific space was built through groupwise registration of T1 and FA images of all individuals [5]. Secondly, the connectivity maps of each subject were propagated to the common space and averaged to get estimates of the group thalamic nuclei location. The obtained priors were then mapped back to each individual's space and used to compute the new connection probability between every thalamic voxel and each cortical region. The steps above were repeated until convergence, and then a thalamus parcellation was obtained.

2.4.2 Proposed strategy (PS): the former segmentation procedure was extended to not only consider tractography and thalamic nuclei priors, but also to incorporate fibre orientation information from each subnuclei. This iterative approach was based on a mixture model of von Mises-Fisher (vMF) and optimised using Expectation-Maximisation (EM). In more detail, it considered:

- **Tractography**: performed as in Section 2.4.1, enables the estimation of six connectivity maps, that describe the connectivity probability of each thalamic voxel to a particular cortical region (prefrontal, motor, sensory, parietal, occipital and temporal). This was represented in the PS as τ;
- **Thalamic nuclei priors**: population-specific and derived following the same steps as in Section 2.4.1. They provide *a priori* information about the expected anatomical connectivity for each thalamic voxel and a specific cortical region, characterised in PS by π;
- **Fibre orientation**: the FOD from each voxel, reconstructed as in Section 2.4.1, was then segmented into its three major fibre orientations using a peak-finding procedure that relies on multiple starting direction points and Newton optimisation [12]. The principal fibre orientation in each voxel was then selected and described in terms of vMF functions.

The diffusion directional data $V = \{v_1, ..., v_N\}$ was modelled by a mixture of c von Mises-Fishers distributions and its probability density function described as:

$$f(v|\theta) = \prod_{i=1}^{N} \sum_{c=1}^{C} \alpha_{ic} f_c(v_i|\theta) \tag{1}$$

The term α_c represents the probability of a certain sample v_i belonging to nucleus c based on information derived from tractography τ and thalamic nuclei priors $\alpha_c = \tau_{ic}.\pi_{ic}$. On the other hand, $f_c(v|\theta_c)$ is a vMF distribution that models the principal fibre orientation in each subnucleus c:

$$f_c(v|\theta) = f_c(v|\mu_c, k_c) = C(k_c) e^{k_c \mu_c^T v} \tag{2}$$

where μ_c is the mean direction, k_c the concentration parameter, $C(k_c) = \frac{k^{1/2}}{(2\pi)^{3/2} I_{1/2}(k_c)}$ the normalisation constant and $I_{1/2}$ the modified Bessel function of the first kind and order 1/2.

The model parameters $\theta = \{\mu_c, k_c\}_{c=1,\ldots,C}$ were learned through a maximum likelihood formulation $\hat{\theta} = \arg\max_\theta L(\theta) = \arg\max_\theta log f(v|\theta)$ and optimised in a iterative way using Expectation-Maximisation (EM) with the following stages:

- E-step: update the membership weights of every element v_i in each cluster c given the parameter set θ at iteration t (θ^t)

$$p(c|v_i, \theta^t) = \frac{\alpha_c f_c(v_i|\theta^t)}{\sum_{c'=1}^{C} \alpha_{c'} f'_c(v_i|\theta^t)} \tag{3}$$

- M-step: find the parameters θ^{t+1} that maximise the expectation of the log likelihood $L(\theta)$

$$r_c = \sum_{i=1}^{N} v_i . p(c|v_i, \theta^t) \tag{4}$$

$$\bar{r}_c = \frac{||r_c||}{\sum_{i=1}^{N} p(c|v_i, \theta^t)} \tag{5}$$

$$\mu_c^{t+1} = \frac{r_c}{||r_c||} \tag{6}$$

$$k_c^{t+1} \approx \frac{3\bar{r}_c - \bar{r}_c^3}{1 - \bar{r}_c^2} \tag{7}$$

The steps above are repeated until convergence. The algorithm returns both $\theta = \{\mu_c, k_c\}_{c=1,\ldots,C}$ which are the parameters of c vMF distributions that model the directional data V, as well the soft-clustering $p(c|v_i, \theta)$ for all c and v_i samples.

3 Results

Thalamus connectivity-based segmentations were derived for the three described strategies (FSL, PW and PS) and individuals – controls and FTD patients – as depicted in Figure 1. The volumes of each connectivity-defined region (CDR) were normalised to the total intracranial volume (TIV) and subsequently compared between the two groups of subjects, in separate for each hemisphere and method, using the Mann-Whitney test. Then, multiple-comparison correction with false discovery rate (FDR) strategy was performed (Table 1).

The PW and PS strategies led to smoother parcellations and more consistent clusters between hemispheres, both in controls and patients, in contrast to FSL (Figure 1). Significant volume differences between controls and patients were observed on the prefrontal CDR in both hemispheres by all the strategies, as shown in Table 1. Additionally, PS and PW were also sensitive to connectivity differences in the temporal CDR, which was not detected with FSL.

4 Discussion and Conclusion

Previously, Behrens et al. [13] developed a probabilistic tractography algorithm and use it to parcellated the thalamus based on its anatomical connectivity towards distinct cortical regions. The resulting segmentations were in agreement with previous known anatomy, with anterior thalamic regions preferentially connected to prefrontal, motor and sensory cortices, whereas posterior clusters had mainly WM projections towards parietal, occipital and temporal regions [14].

This aspect was also evident on the thalamus parcellations generated by PW and PS approaches, both on normal controls and FTD patients, which did not occur with the segmentations derived with FSL, as depicted in Figure 1.

The connectivity differences detected by PS and PW were in concordance with previous FTD studies that have reported volume differences both on prefrontal and temporal cortices [15, 16], while FSL was only able to pick on the prefrontal region (Table 1).

PW and PS strategies rely both on tractography and thalamic nuclei priors, but additionally PS accounts for the local fibre orientation. Similar results were obtained with these approaches both in terms of the generated segmentations (Figure 1) and volume comparisons with identical p-values (Table 1). The incorporation of fibre orientation by PS may not seem an obvious advantage, but

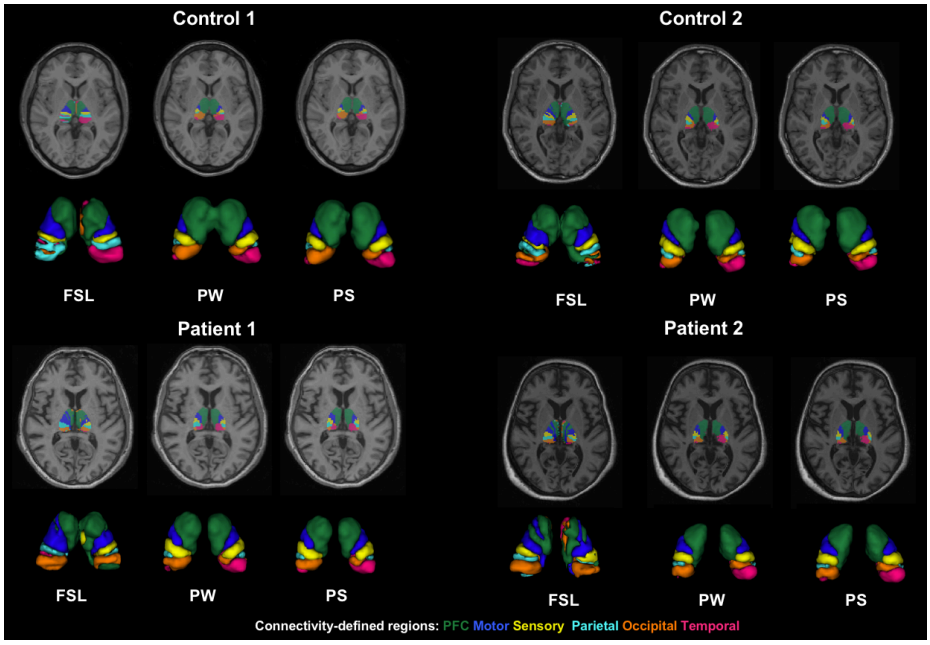

Fig. 1. Thalamic nuclei segmentations generated by FSL, PW and PS in four example individuals displayed in MNI152 space.

Left hemisphere						
Method	**Prefrontal**	**Motor**	**Sensory**	**Parietal**	**Occipital**	**Temporal**
FSL	0.039*	0.992	0.840	0.651	0.992	0.110
PW	0.014*	0.406	0.705	0.853	0.705	0.014*
PS	0.014*	0.496	0.555	0.799	0.250	0.016*
Right hemisphere						
Method	**Prefrontal**	**Motor**	**Sensory**	**Parietal**	**Occipital**	**Temporal**
FSL	0.039*	0.947	0.625	0.625	0.947	0.794
PW	0.012*	0.904	0.794	0.687	0.236	0.019*
PS	0.012*	0.947	0.936	0.625	0.035	0.019*

Table 1. Corrected FDR p-values obtained by comparing the normalised CDRs volumes between controls and FTD patients groups. Significant volumes differences were detected on the prefrontal CDR in both hemispheres with all strategies, whereas for the temporal CDR this was just observed with PW and PS approaches (one-tailed significance test and $P<0.05$).

it complements the global connectivity information obtained with tractography, and hence guarantees a better subdivision of the thalamus. This is particularly relevant in the posterior thalamic region as it is a fibre-crossing area, so the anatomical connectivity reconstruction is more challenging.

Further validation of these results may involve a bigger cohort, as well the performance of reproducibility tests. Future work will enhance the proposed strategy by including other relevant modalities and geometrical constraints in order to generate better thalamic nuclei segmentations and priors, and extend the technique to the study of other neurological pathologies.

Acknowledgements This research was funded by the EPSRC UCL Centre for Doctoral Training in Medical Imaging (EP/L016478/1), NIHR BRC UCLH/UCL High Impact Initiative and Icometrix industrial partner. The Dementia Research Centre is supported by Alzheimer's Research UK, Brain Research Trust, and The Wolfson Foundation. This work was funded by the NIHR Queen Square Dementia Biomedical Research Unit, the NIHR UCL/H Biomedical Research Centre and the Leonard Wolfson Experimental Neurology Centre (LWENC) Clinical Research Facility as well as an Alzheimer's Society grant (AS-PG-16-007). JDR is supported by an MRC Clinician Scientist Fellowship (MR/M008525/1) and has received funding from the NIHR Rare Disease Translational Research Collaboration (BRC149/NS/MH). This work was supported by the MRC UK GENFI grant (MR/M023664/1) and by The Bluefield Project. CHS receives support from the Alzheimers Society (AS-JF-17-011).

References

1. Behrens, T.E.J., Berg, H.J., Jbabdi, S., Rushworth, M.F.S., et al.: Probabilistic diffusion tractography with multiple fibre orientations: What can we gain? NeuroImage **34**(1) (2007) 144–155
2. Semedo, C., Cardoso, M.J., Vos, S.B., et al.: Improved tractography-based segmentation of the human thalamus. Proceedings of the International Society for Magnetic Resonance in Medicine (2017)
3. Semedo, C., Cardoso, M.J., Vos, S.B., et al.: Thalamic nuclei segmentation on dementia using tractography and population-specific priors. Proceedings of the International Society for Magnetic Resonance in Medicine (2018)
4. Tustison, N.J., Avants, B.B., Cook, P.A., et al.: N4ITK: Improved N3 Bias Correction. IEEE Transactions on Medical Imaging **29**(6) (2010) 1310–1320
5. Modat, M., Ridgway, G.R., Taylor, Z.A., et al.: Fast free-form deformation using graphics processing units. Computer Methods and Programs in Biomedicine **98**(3) (2010) 278–284
6. Daga, P., Pendse, T., Modat, M., White, M., et al.: Susceptibility artefact correction using dynamic graph cuts: Application to neurosurgery. Medical Image Analysis **18**(7) (2014) 1132–1142
7. Jenkinson, M., Bannister, P., Brady, M., Smith, S.: Improved optimization for the robust and accurate linear registration and motion correction of brain images. NeuroImage **17**(2) (2002) 825–841
8. Klein, A., Andersson, J., Ardekani, B.A., Ashburner, J., et al.: Evaluation of 14 nonlinear deformation algorithms applied to human brain MRI registration. NeuroImage **46**(3) (2009) 786–802
9. Cardoso, M.J., Modat, M., Wolz, R., et al.: Geodesic Information Flows: Spatially-Variant Graphs and Their Application to Segmentation and Fusion. IEEE Transactions on Medical Imaging **34**(9) (2015)
10. Tournier, J.D., Calamante, F., Connelly, A.: Robust determination of the fibre orientation distribution in diffusion MRI: Non-negativity constrained super-resolved spherical deconvolution. NeuroImage **35**(4) (2007) 1459–1472
11. Tournier, J.D., Calamante, F., Connelly, A.: Improved probabilistic streamlines tractography by 2nd order integration over fibre orientation distributions. Proceedings of the International Society for Magnetic Resonance in Medicine **18** (2010) 1670
12. Jeurissen, B., Leemans, A., Tournier, J.D., Jones, D.K., Sijbers, J.: Investigating the prevalence of complex fiber configurations in white matter tissue with diffusion magnetic resonance imaging. Human Brain Mapping **34**(11) (2013) 2747–2766
13. Behrens, T.E.J., Johansen-Berg, H., Woolrich, M.W., et al.: Non-invasive mapping of connections between human thalamus and cortex using diffusion imaging. Nature neuroscience **6**(7) (2003) 750–757
14. Catani, M., Thiebaut De Schotten, M.: Atlas of Human Brain Connections. Oxford University Press (2012)
15. Rohrer, J.D., Nicholas, J.M., Cash, D.M., et al.: Presymptomatic cognitive and neuroanatomical changes in genetic frontotemporal dementia in the Genetic Frontotemporal dementia Initiative (GENFI) study: A cross-sectional analysis. The Lancet Neurology **14**(3) (2015) 253–262
16. Cardenas, V.A., Boxer, A.L., Chao, L.L., et al.: Deformation-based morphometry reveals brain atrophy in frontotemporal dementia. Archives of neurology **64**(6) (2007) 873–877